

The effect of diffusion barrier formation on the kinetics of aluminizing in inconel-718

V. SHANKAR, A. L. E. TERRANCE, S. VENKADESAN
*Metallurgy and Materials Group, Indira Gandhi Centre for Atomic Research,
 Kalpakkam 603 102, India*

J. ANNAPURNA
Defence Metallurgical Research Laboratory, Kanchanbagh, Hyderabad 500 258, India

Aluminizing of nickel alloy 718 was studied in order to reveal the effect of combined alloy additions on aluminide growth kinetics, as opposed to pure metal substrates. The low activity pack process was used and treatment was carried out at 1273 K using ammonium fluoride activator and Ni–50 wt% Al powder as an aluminium source for treatment times of 1, 2, 4 and 8 h. The aluminide coatings varied between 40 and 110 μm in thickness. The microstructures consisted of a NiAl phase with a fine grain size containing small secondary-phase particles at the grain boundaries. The interface between the coating and the substrate was lined by a lamellar layer exhibiting a two-phase structure, which was enriched in chromium and niobium in addition to containing iron and nickel. Weight gain measurements indicated parabolic growth up to 2 h, beyond which the growth rate slowed down. Microstructures and composition profiles revealed that the interlayer, which was enriched in elements insoluble in NiAl, posed a barrier to interdiffusion of the reacting species and slowed down the growth kinetics of the aluminide.

1. Introduction

Aluminide coatings of the NiAl type are used to protect components of nickel- and iron-based alloys operating in oxidizing environments [1, 2]. The coatings also exhibit very high hardness and stability under impact fretting and adhesive wear situations and are therefore used for wear-resistant applications in liquid-metal cooled fast breeder reactors [3]. Aluminizing is usually carried out by the pack-cementation process in which the component to be coated is treated at temperatures between 1073 and 1423 K in a pack consisting of an aluminium source, an activator and alumina filler. Goward [1] and Goward and Boone [2] studied the formation of aluminide coatings and made a distinction between two types of coating processes based on the source being either unalloyed aluminium (aluminium at unit activity) or aluminide powders (aluminium activity less than 1). The processes are referred to as “high” and “low” activity pack processes, respectively.

Several studies have been conducted on the kinetics of aluminization from pure aluminium packs [4, 5], as well as in alloy packs of varying aluminium activity [6, 7]. From earlier studies, it has been clarified that the reactions occurring during aluminizing can be assumed to take place in three stages: (1) reactions between carrier gases (aluminium halides) on the powder and specimen surfaces; (2) diffusion of carrier gases from the pack to the specimen surface; and (3) solid-state diffusion of substrate species and alumi-

num resulting in coating growth. Of the above three processes the surface reactions are reported to take place much faster than the solid- and gas-phase diffusion steps [4, 6, 7]. When the supply of aluminium from the gaseous phase is freely available, solid-state diffusion has been found to control the growth rate and a parabolic relationship has been observed between the weight gain and the aluminizing time [4, 5]:

$$w = (kt)^{1/2}$$

The addition of alloying elements to pure nickel is known to change the growth behaviour of the aluminide coatings. When the nickel content in the substrate is decreased the parabolic growth constant decreases with respect to that in pure nickel [5]. An increase in the chromium content in the substrate has also been found to decrease the growth constant at temperatures between 1273 and 1373 K [5]. Further, continuous or semi-continuous interlayers are known to form [4, 5] between the substrate and the coating during the aluminizing of superalloys containing elements such as Cr, Mo, Nb, W, etc., which show poor solubility in the NiAl phase. While it is known that these layers contribute to the thermal stability of the coating and improved oxidation resistance in service by acting as diffusion barriers [1, 2, 5], the influence of the barrier layers on the kinetics of the aluminizing process itself has not been widely reported. In the present work the kinetics of aluminization of nickel alloy 718 by the low activity pack aluminizing process has been studied

and the probable influence of the diffusion barrier on aluminizing kinetics is discussed.

2. Experimental procedure

Specimen coupons of alloy 718 measuring $2 \times 10 \times 12$ mm were treated for various times in a pack consisting of an aluminium source, an activator and an alumina filler using pre-aluminized nickel-base alloy retorts. The composition of the alloy 718 was: 53.5% Ni, 18.5% Cr, 19.5% Fe, 5% Nb, 3% Mo, 1% Ti and 0.065% C. Ammonium fluoride at 2% of the pack weight was used as the activator. The aluminium source was Ni-50 wt % Al (68 a/o) alloy powder at 25% of the pack composition, the remainder being alumina powder. Treatments were carried out at 1273 K for times of 1, 2, 4 and 8 h, an argon atmosphere was maintained inside the furnace during treatment. The furnace was a tubular type with extensions on either side of the hot zone to hold the specimen boat in the argon atmosphere during cooling after treatment.

Three specimen coupons were aluminized for each treatment time. Specimens were weighed before and after treatment to determine the weight gain. Treated specimens were examined by optical microscopy and elemental profiles were obtained by electron-probe

microanalysis. The σ/k values during elemental profiling were less than 1 at % for Al, Ni, Cr and Fe across the specimen. The microstructures for optical microscopy were revealed by electrolytically etching in a solution of 5% hydrofluoric acid, 10% glycerol and 85% water at 5 V for a few seconds. X-ray diffraction analysis (XRDA) of the samples was done to reveal the phases present. Microhardness measurements were made on metallographically prepared specimens.

3. Results and discussion

3.1. Coating microstructures

Optical microstructures of aluminide coatings on alloy 718 for various treatment times are shown in Fig. 1. The thickness of the aluminide layers obtained varied from 40 to 50 μm in the 1 h treatment to 110 μm in the 8 h treatment. As observed in Fig. 1, the coatings consisted of a NiAl phase of very fine grain size (less than 5 μm) near the surface of the coating which increased to 10–15 μm in the interior of the coating. Fine second-phase particles were observed at the grain boundaries of the fine-grained zone, indicating their pinning effect on the boundaries. Fewer second-phase particles were present in the interior of the coating, which resulted in grain growth, particularly in the 8 h specimen (Fig. 1d). Some particles were found in the

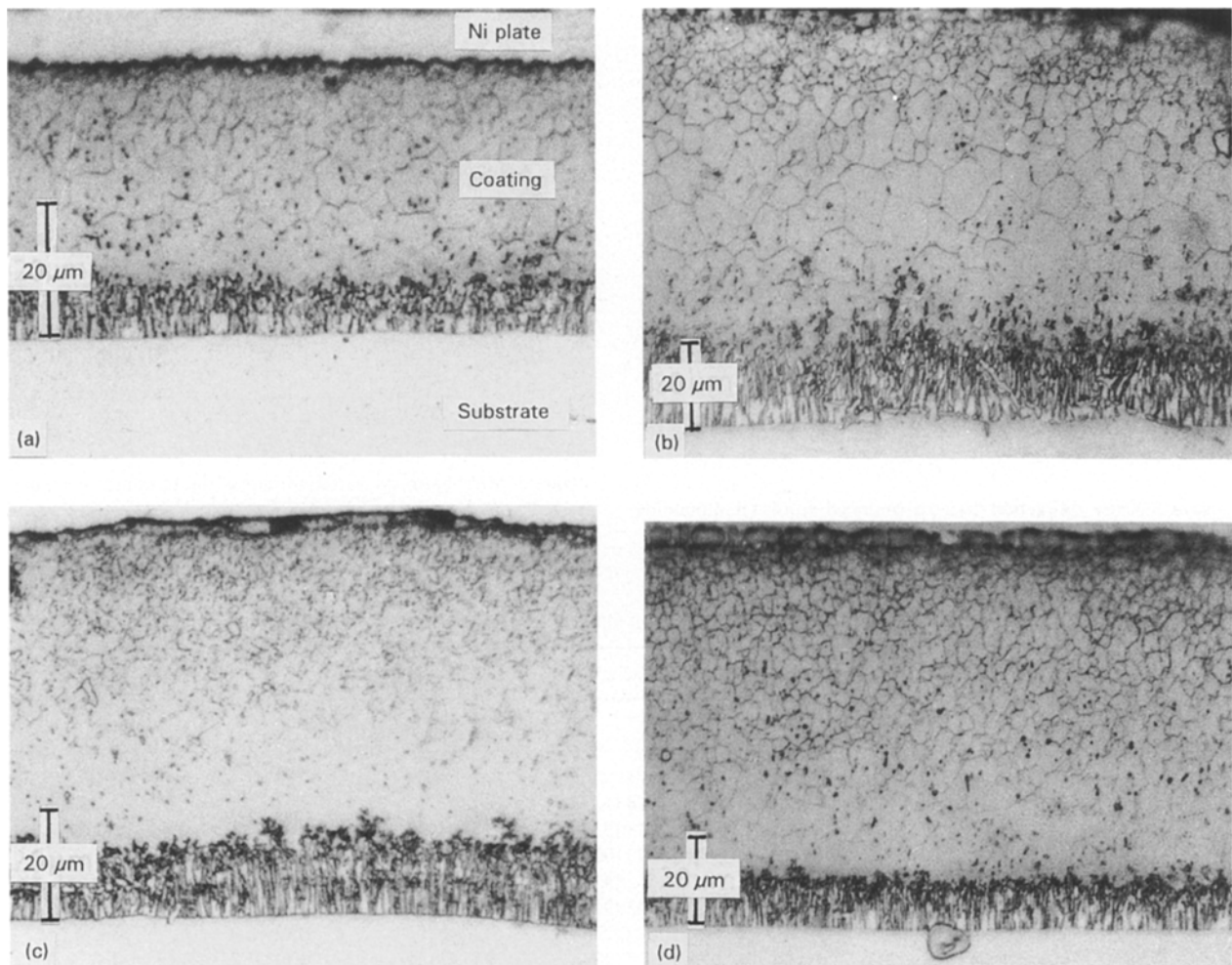


Figure 1 Optical micrographs of low activity pack-aluminide coatings on alloy 718 for various treatment times (h): (a) 1; (b) 2; (c) 4; (d) 8.

grain interiors also. The boundary between the aluminate and the substrate was lined by an interlayer exhibiting a two-phase lamellar structure (Fig. 1). The thickness of the interlayer was ca. 10 μm in the 1 h specimen (Fig. 1a), which increased to 25–30 μm in the 8 h specimen (Fig. 1d). It was evident that the secondary-phase particles in the coating resulted from breakup of the lamellae, which was observable in the aluminate close to the interlayer. The microstructural features of the coating, such as precipitation and the lamellar interlayer, obtained in the present work were similar to those found by Slattery [8].

XRDA of the four coatings revealed that the major phase present was of the NiAl type, as observed in Fig. 2. The d -spacings of the major peaks are listed in Table I, where it is observed that the peaks generally corresponded to NiAl, although both the peak positions and the intensities can be considered intermediate between those of NiAl and FeAl. Lattice parameters calculated from the patterns showed the values to lie between those of NiAl (0.288 nm) and FeAl (0.290 nm). The d -spacings for the four treatment times did not show a significant or systematic variation. Any minor phases present could not be clearly identified, except possibly for σ (FeCr), due to the small volume fraction present. The coatings exhibited very high hardness, ca. 900 H_V , as seen in Fig. 3, and the values were nearly the same for all the treatment times.

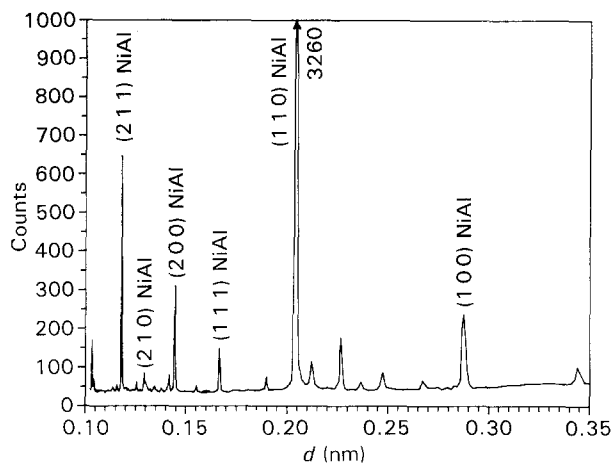


Figure 2 X-ray diffraction pattern obtained from 1 h aluminate coating.

3.2. Composition of the coating

The composition profiles of the 1, 4 and 8 h coatings obtained by electron probe microanalysis are shown in Figs 4–6. In the 1 h coating (Fig. 4) the aluminium concentration decreased steeply, while that of nickel increased before decreasing sharply in the interlayer. The profiles of iron and chromium are similar. The iron content was virtually constant, while chromium decreased slightly close to the interlayer. Nb, Mo and Ti were present in very low concentrations in the aluminate layer. In the 4 h coating (Fig. 5) the decrease in the Al content was more gradual as a function of depth, while Ni showed an increase, as with the 1 h coating. The profiles of Fe and Cr and those of Nb, Mo and Ti were similar to that of the 1 h coating. When the coating time was increased to 8 h the Al content remained nearly constant (Fig. 6), the peak in the nickel content near the interlayer was absent. There was no qualitative change in the profiles of the rest of the elements between the three cases.

The surface aluminium content of low-activity pack aluminized specimens has been studied as a function of aluminizing time and pack composition by Sivakumar and Seigle [6] for nickel, and by Wang and Seigle [7] for iron substrates. They found that the surface aluminium content attained a steady-state with respect to time for a given pack composition. In the present case the elemental profiles show that the surface aluminium concentration was nearly invariant

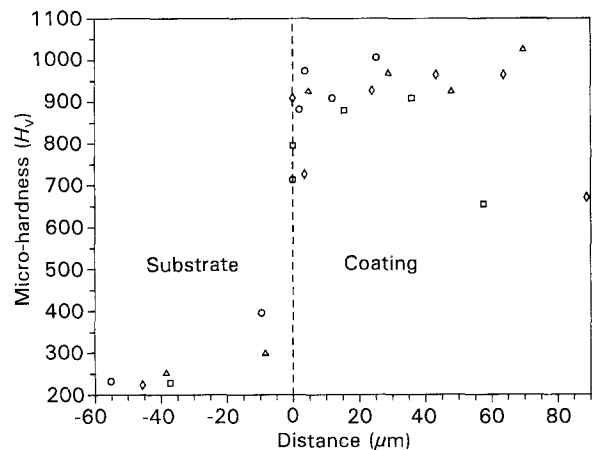


Figure 3 Microhardness variation across the interface of aluminized alloy 718 specimens. Aluminizing time (h): \circ , 1; \square , 2; \triangle , 4; \diamond , 8.

TABLE I XRD data for low activity pack aluminate coatings on alloy 718 for various treatment times^a

Sample No.	NiAl	FeAl	d -Spacings (nm)			
			1 h	2 h	4 h	8 h
1	0.287 (40)	0.289 (12)	0.287 (7.2)	0.2884 (5.8)	0.2875 (7.5)	0.2893 (6)
2			0.2264 (5.3)	0.2267 (4.8)	0.2263 (4.9)	0.227 (3)
3			0.2118 (3.5)	0.212 (4.2)	0.2117 (3.2)	0.2126 (3 –)
4	0.202 (100)	0.204 (100)	0.204 (100)	0.204 (100)	0.2039 (100)	0.2043 (100)
5	0.1655 (20)	0.167 (4)	0.1655 (4.5)	0.1666 (3.6)	0.1665 (4.2)	0.1667 (3.5)
6	0.1434 (20)	0.145 (8)	0.1443 (9.33)	0.1444 (7.8)	0.1441 (8.8)	0.1445 (7.7)
7	0.1285 (10)	0.130 (3)	0.129 (2.5)	0.1292 (tr)	0.129 (tr)	0.1291 (tr)
8	0.1171 (70)		0.1177 (20)	0.1179 (20)	0.1177 (23)	0.1179 (17)

^a Figures in parentheses are the percentage intensities.

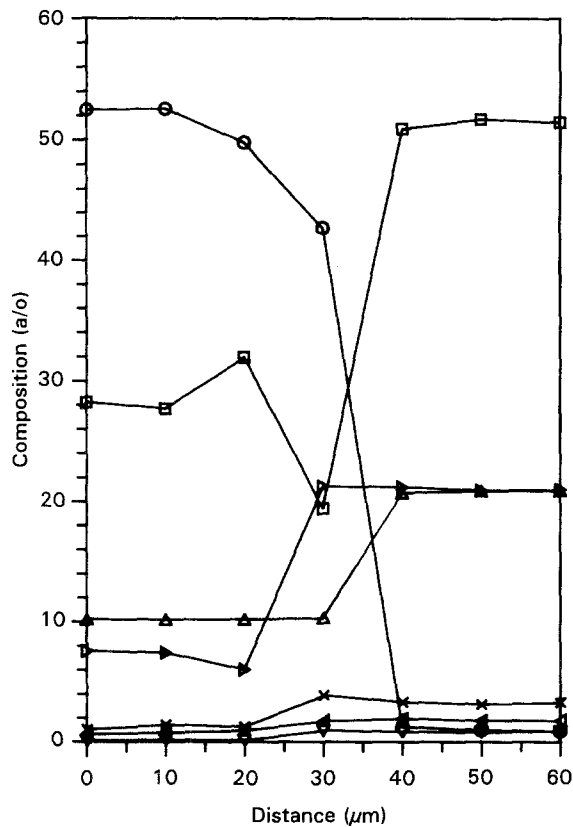


Figure 4 Elemental composition profiles obtained across a specimen aluminized for 1 h. ○, Al; □, Ni; △, Fe; ◇, Cr; ×, Nb; ▽, Ti; ◁, Mo.

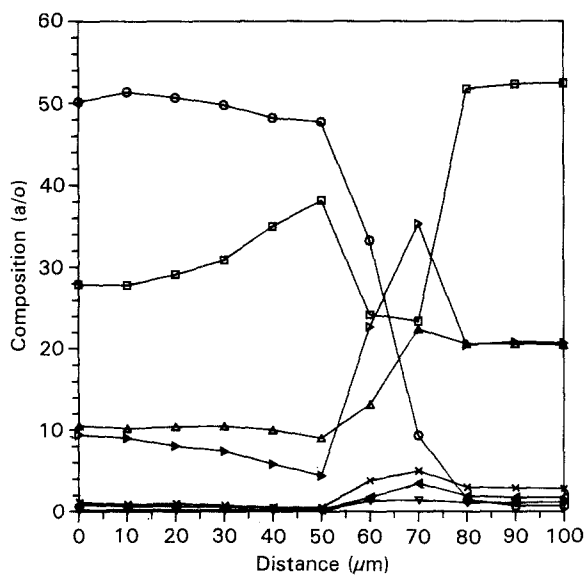


Figure 5 Elemental composition profiles obtained across a specimen aluminized for 4 h. ○, Al; □, Ni; △, Fe; ◇, Cr; ×, Nb; ▽, Ti; ◁, Mo.

(52 at %) in the three coatings, implying a steady-state situation with respect to aluminium availability from the pack to the surface of the aluminide layer.

The XRD patterns and the composition profiles show that the structure of the aluminide was that of NiAl (B2 structure) with about 20 at % of iron and chromium substituted in nearly equal amounts in the nickel sites of the B2 structure. The variation in elemental concentrations across the coating were very

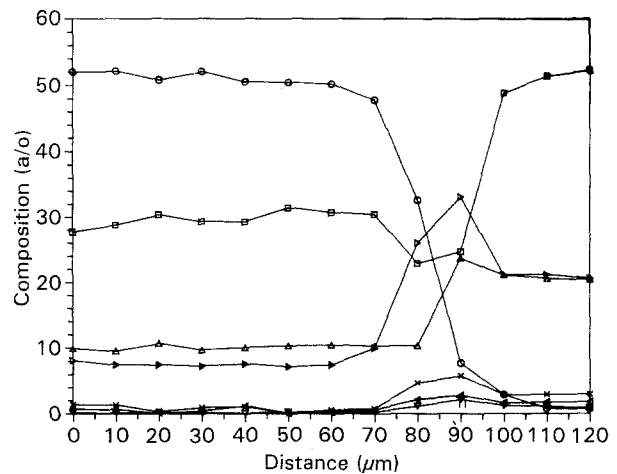


Figure 6 Elemental composition profiles obtained across a specimen aluminized for 8 h. ○, Al; □, Ni; △, Fe; ◇, Cr; ×, Nb; ▽, Ti; ◁, Mo.

similar to those obtained by Slattery [8] in Inconel-718. An increase in nickel content in the coating near the interlayer and the slight decrease in iron and chromium contents approaching the interlayer, as evident in the 1 and 4 h specimens, were similar.

3.3. Composition of the interlayer

The aluminium profile shows a sharp decrease in the interlayer of the 1 h coating, and the nickel level in this layer was less than both the aluminide and the substrate levels. Both iron and chromium and the minor alloying elements Nb, Mo and Cr showed increased concentrations in the interlayer when compared to both the aluminide and the base metal. In the 4 h coating aluminium showed a sharp decrease to low values while nickel decreased to ca. 24 at % from 40 at % in the aluminide. Both chromium and iron increased in the interlayer, with a peak in both elements close to the substrate side. The chromium content was observed to be much higher than that in the substrate and the coating. In the 8 h specimen the profiles of all the elements across the interlayer were similar to those of the other treatment times. In summation, the interlayer showed an enrichment in Cr, Fe, Nb, Mo and Ti and a steeply decreasing aluminium concentration.

3.4. Kinetics and mechanism of aluminide growth on alloy 718

The specific weight gain of the specimens is shown as a function of $t^{1/2}$ in Fig. 7. It is observed that the weight gain was rapid and parabolic in the 1 and 2 h specimens, but the rate of weight gain tapered off beyond 2 h in the 4 and 8 h specimens. Metallographic measurements of coating thickness indicated a similar trend. Such a decrease in the growth rate during aluminizing has not been previously reported.

It has been observed that in alloys containing chromium and other elements insoluble in the aluminide phase, the coating growth rate decreases in proportion to the content of those elements. According to

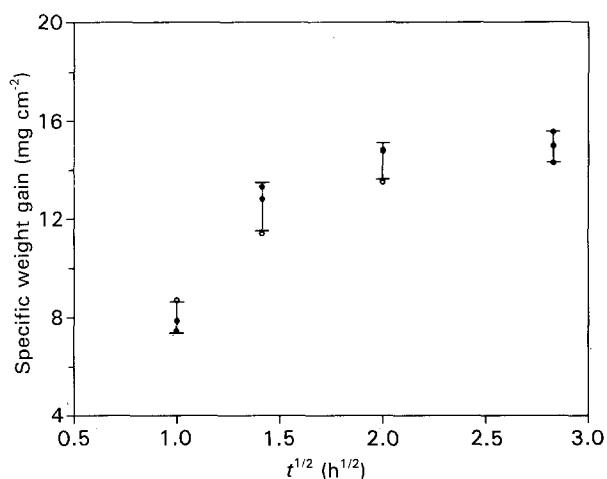


Figure 7 Specific weight gains obtained as a function of treatment time during aluminizing of nickel alloy 718.

Fitzer and Maurer [5], increasing the chromium content in a nickel-based matrix from 10 to 30% decreased the growth rate constant by more than one order of magnitude, due to the formation of a Cr–Ni interlayer across which both nickel and aluminium transport were greatly reduced. In the present case, the change in growth rate of the coating may be correlated with the increasing concentration of chromium and niobium in the interlayer, from ca. 25 at % in the 1 h coating to 40 at % beyond 4 h. The increase in the thickness of the interlayer at longer treatment times would also decrease the diffusion path available for diffusion of both nickel and aluminium through this layer.

In aluminizing nickel, it is known that the mechanism of coating growth is through the inward diffusion of aluminium in aluminium-rich NiAl, while that in nickel-rich NiAl is due to outward diffusion of nickel from the substrate into the aluminide. The inward diffusion coating is identified by *in situ* precipitation of insoluble elements, while when outward diffusion takes place the elements insoluble in the aluminide are left behind at the coating–substrate interlayer and a relatively precipitate-free region is present between the interlayer and the outer zone of the coating. The microstructures due to the two types of growth mechanism have been discussed by Goward and Boone [2]. In the present case, the coating composition is slightly aluminium-rich. In Fig. 1a–d the uniform distribution of precipitates near the surface of the coatings, which resulted in a fine grain size, is likely to have been caused by inward diffusion of aluminium and consequent *in situ* precipitation of the insoluble elements. Further growth of the coating proceeded with significantly less precipitation, indicating that the nickel required was obtained by diffusion outward from the matrix through the interlayer, which had been enriched in chromium and niobium due to nickel depletion in the underlying matrix. The de-

crease in the coating growth rate was accompanied by a change in the controlling mechanism from inward aluminium diffusion in the 1 and 2 h specimens to outward nickel diffusion in the 4 and 8 h specimens. The low aluminium content of the interlayer, particularly in the 4 and 8 h specimens, and the steep drop in aluminium content across it, suggests that it is very effective in preventing aluminium diffusion into the substrate and that the growth of the aluminide is dependent on nickel diffusion outward from the substrate through the interlayer.

4. Conclusions

The results of the present work show that

1. The formation of a chromium–niobium-rich diffusion barrier layer during the aluminizing of nickel alloy 718 slowed down the growth kinetics of the aluminide as a function of aluminizing time.
2. The mechanism of coating formation was initially inward diffusion of aluminium into the substrate, while formation of the diffusion barrier resulted in further growth due to outward diffusion of nickel from the substrate through the barrier.
3. The aluminium content of the barrier layer decreased sharply across its thickness, while the nickel content remained fairly uniform. The barrier layer was composed of phases containing high concentrations of chromium, niobium and iron, besides nickel.

Acknowledgements

The authors acknowledge the keen interest shown by Drs P. Rodriguez and S. L. Mannan in the course of this study. This work would not have been possible but for the experimental facilities and help received from Dr R. Sivakumar for carrying out the aluminizing experiments at DMRL, Hyderabad.

References

1. G. W. GOWARD, *J. Metals* **22** (1970) 31.
2. G. W. GOWARD and D. H. BOONE, *Oxidation of Metals* **3** (1971) 475.
3. M. W. J. LEWIS and C. S. CAMPBELL, in "Liquid metal engineering and technology", Vol. 1 (BNES, London, 1984) p. 91.
4. S. R. LEVINE and R. M. CAVES, *J. Electrochem. Soc.* **121** (1974) 1051.
5. E. FITZER and H. J. MAURER, in "Materials and coatings to resist high temperature corrosion", edited by D. R. Holmes and A. Rahmel (Applied Science, London, 1978) p. 253.
6. R. SIVAKUMAR and L. L. SEIGLE, *Metall. Trans.* **7A** (1976) 1073.
7. T. H. WANG and L. L. SEIGLE, *Mater. Sci. Engng.* **A108** (1989) 253.
8. G. F. SLATTERY, *Metals Technol.* **10** (1983) 41.

Received 25 March 1993
and accepted 21 April 1994